

INVITED SESSION NUMBER: 157

Event-Based Feedback Control of Nonlinear Oscillators Using Phase Response Curves

Per Danzl and Jeff Moehlis

Abstract—The phase response curve for a nonlinear oscillator describes the phase-shift of the oscillation due to an impulsive perturbation as a function of the phase at which the perturbation occurs. We propose a novel feedback control mechanism which allows one to control the phase of an oscillation, assuming only that the phase response curve is known and that a once-per-period marker event, such as the time at which a neuron fires, can be detected. The effectiveness of this control method is demonstrated through analytical and numerical results. This work represents a first step toward a closed-loop form of electrical deep brain stimulation, a treatment for neuromotor disorders such as Parkinson’s disease, with symptoms characterized by pathological neural synchronization.

I. INTRODUCTION

Symptoms of neuromotor disorders, such as Parkinson’s Disease (PD), have been linked to pathological synchronization of neuronal signals, which consist of sequences of voltage spikes, or *action potentials* [11],[4]. Such disorders may be treated by a surgically implanted device, similar to a cardiac pacemaker, that sends a high frequency electrical stimulus into the motor control region of the brain, specifically the thalamus. This treatment, known as Electrical Deep Brain Stimulation (EDBS), has been successful in alleviating the symptoms of a variety of diseases including neuromotor disorders, obsessive-compulsive disorder, and even depression [1]. Since its approval by the FDA in 1997 for use in advanced cases of PD, and in 2003 for dystonia, EDBS therapy has helped thousands of patients increase their quality of life. The treatment, however, causes side-effects including collateral damage to surrounding brain tissue due to the continuous application of the stimulus signal, which leads to dysarthria, dysesthesia, and cerebellar ataxia [13].

Researchers in the neuroscience community have become interested in the concept of “Demand-Controlled” EDBS. It has been argued that the side-effects of electrical stimulation can be minimized by applying the stimulus only when synchronization is detected [13]. We view this essentially as a feedback control problem, and direct our first efforts toward the task of controlling the firing times of a single oscillatory neuron (a participant in the pathological synchronized oscillatory population dynamics).

This work is supported by a Sloan Research Fellowship in Mathematics and National Science Foundation grant NSF-0547606

P. Danzl and J. Moehlis are with the Department of Mechanical Engineering, University of California, Santa Barbara CA, 93106 {pdanzl,moehlis}@engineering.ucsb.edu

In this paper, we seek a closed-loop control law that, based on the detection of a voltage spike, drives an oscillatory neuron to track a periodic reference phase trajectory using a charge-balanced control signal (to avoid accumulation of charge in the tissue). In the limit of weak coupling, we envision a set of such controllers driving a population of oscillating neurons to track time-staggered reference trajectories, achieving desynchronization.

II. PROBLEM STATEMENT

We consider a population of uncoupled phase oscillators, derived from conductance-based neuron models, that are each equipped with both a stimulus and feedback electrode. We seek to develop a control law that results in a uniform (desynchronized) phase distribution around $\mathbb{S}^1 = [0, 2\pi)$, based only on the detection of once-per-period marker events (action potentials) of the individual oscillators.

A. Individual Neuron Models

The dynamics of neuronal membrane voltage signals are typically modeled using conductance-based ordinary differential equation systems, following the Hodgkin-Huxley formalism [7], in the space-clamped form

$$C\dot{V} = I_g(V, \mathbf{n}) + I_b + I(t), \quad \dot{\mathbf{n}} = \mathbf{G}(V, \mathbf{n}),$$

where $V \in \mathbb{R}$ is the voltage across the membrane, $\mathbf{n} \in \mathbb{R}_{[0,1]}^m$ is the vector of gating variables, C is the constant membrane capacitance, $I_g : \mathbb{R} \times \mathbb{R}^m \rightarrow \mathbb{R}$ is the sum of the membrane currents, $I_b \in \mathbb{R}$ is a constant baseline current, and $I : \mathbb{R} \rightarrow \mathbb{R}$ is the stimulus current. It is notable that the Hodgkin-Huxley equations themselves are a feedback-connected system.

We assume the neuron is operating in a region of parameter space such that there exists a stable periodic orbit, $\mathbf{x}^\gamma(t)$, with natural frequency ω . Following [2], [3], we introduce phase variable $\theta(\mathbf{x}) : \mathbb{R}^{m+1} \rightarrow [0, 2\pi)$ such that, in the absence of input $I(t)$, we have $\dot{\theta} = \omega$. Let $\theta = 0$ correspond to a marker event - the peak value of V on periodic orbit $\mathbf{x}^\gamma(t)$, i.e. the action potential. With input,

$$\dot{\theta} = \omega + \frac{Z_V(\theta)}{C} I(t), \quad (1)$$

where $Z_V(\theta) \in \mathbb{R}$ is the voltage component of the phase response curve (PRC) $Z(\theta) \in \mathbb{R}^{m+1}$, computed by solving an adjoint equation, as described, e.g., in [2]. Originally proposed by [15], [16], the concept of phase reduction

was formalized mathematically in [5] in the limit of *small* perturbations, which fits in well with the present control objective of minimizing stimulus energy. We endeavor to show that the information contained in the phase response curve provides a means to develop feedback-based control schemes that achieve our desynchronization objective for a class of conductance-based neuron models that undergo a Hopf (or Bautin) bifurcation to a stable periodic orbit. Members of this class include the Hodgkin-Huxley system [7], and its FitzHugh-Nagumo reduction [8]. Figure 1 shows the voltage component of the phase response curve for the Hodgkin Huxley system for a typical oscillatory parameter set [2], which is qualitatively similar to the simplest phase oscillator representation of this class:

$$\dot{\theta} = \omega - \sin(\theta)u(t). \quad (2)$$

This corresponds to (1) with $Z_V = -\sin(\theta)$, $I(t)/C = u(t)$, where the capacitance C of the system is a constant, usually taken to equal 1. We will focus on this simplified oscillator in order to simplify the development of the forthcoming convergence results. Then we will extend our results to more general phase response curves of this class.

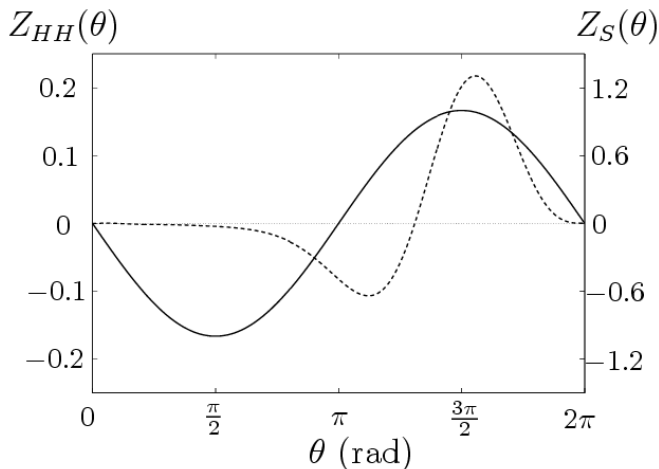


Fig. 1. Phase response curves. The dashed line represents the space-clamped Hodgkin-Huxley system $Z_{HH}(\theta)$ with a baseline current of 10mA. The solid line is the simple $Z_S(\theta) = -\sin(\theta)$.

B. Observables

We impose the constraint that the only observable for each neuron model is the detection of a voltage spike (action potential). This is based on the fact that membrane voltage measurements are quite noisy, and ionic gates are impossible to measure *in vivo*. By limiting ourselves to a simple measurable observable, such as the occurrence of an action potential, we ensure that the control concepts developed will be applicable to the physical system.

C. Population Model

In this very simplified scenario of uncoupled oscillators, the ability to independently control many single oscillators to match a set of reference phase trajectories is equivalent

to the ability to desynchronize the population. To quantify synchrony, we follow [9] and introduce the *order* parameter

$$Re^{i\Psi} = \frac{1}{N} \sum_{j=1}^N e^{i\theta_j}, \quad (3)$$

where N is the number of oscillators and $R \in [0, 1]$ quantifies the level of synchrony of the first (primary) mode. At the population level, our control objective is to drive R to zero. This objective will be achieved if we are able to drive each oscillator to a corresponding staggered reference trajectory

$$\theta_{rj}(t) = \omega t + \theta_{rj}(0) \pmod{2\pi}, \quad (4)$$

where $\theta_{rj}(0) = \frac{j-1}{N}2\pi$, since this set of reference trajectories satisfies

$$\text{Re} \left(\frac{1}{N} \sum_{j=1}^N e^{i(\omega t + \frac{j-1}{N}2\pi)} \right) = 0 \quad \forall t \geq 0. \quad (5)$$

Following this argument, we will now focus on the single oscillator case.

III. REFERENCE TRACKING CONTROL

For the phase oscillator represented by (2), we propose a simple charge-balanced waveform and show that there exist parameters such that the proposed waveform contracts the phase error over one period of oscillation, which implies monotonic global convergence of the oscillator phase to a fixed reference phase with the same frequency.

We define the phase error of an oscillator relative to the reference phase θ_r by

$$\Delta\theta = \begin{cases} \theta_r - \theta & , \quad \text{for } |\theta_r - \theta| \leq \pi \\ \theta_r - \theta - \text{sgn}(\theta_r - \theta)2\pi, & \text{for } |\theta_r - \theta| > \pi \end{cases} \quad (6)$$

where θ is the phase of the oscillator. This non-standard definition of error is made so that a positive error means the neuron needs to speed up, and a negative error means that it must slow down to correct the error.

Since the only observable is a voltage spike, which we define to be $\theta = 0$, we propose a controller that updates each time the oscillator spikes, and forms a stimulus waveform based on a snapshot of the phase error $\Delta\theta = \theta_r$ computed when the oscillator spikes. We wrap this error so that $\Delta\theta \in (-\pi, \pi]$, which allows the controller to either slow the neuron down or speed it up to match the appropriate reference spike. For the following theorem, we take the time duration of the action of the controller waveform to be

$$t_s = (2\pi - |\Delta\theta|/2)/\omega. \quad (7)$$

In this simple case, the PRC $Z_S(\theta) = -\sin(\theta)$ has zero crossings at $\theta = 0$ and $\theta = \pi$. A simple charge-balanced waveform which guarantees contraction is the piecewise constant function

$$u(t) = \begin{cases} u_1, & \text{for } t_0 \leq t < t_0 + t_s/2 \\ u_2, & \text{for } t_0 + t_s/2 \leq t < t_0 + t_s \\ 0, & \text{otherwise} \end{cases} \quad (8)$$

where $u_1 = -c\Delta\theta$, $u_2 = c\Delta\theta \equiv \bar{u}$, and t_0 is the time of the last oscillator spike, which by translating time for each control period, we may take as zero. This is, in a sense, a kind of discrete proportional control scheme, where the magnitude of the control stimulus is proportional to the phase error calculated each time the oscillator passes through its marker event at $\theta = 0$. The following result proves that this control scheme reduces the phase error in the limit of small stimuli.

Theorem For the oscillator $\dot{\theta} = \omega - \sin(\theta)u(t)$ where $u(t)$ is as defined above with $\bar{u} = c\Delta\theta$, the phase error $\Delta\theta$ of the oscillator will be a contraction in the limit of small, positive c .

It is worthwhile to note that this theorem implies global monotonic convergence of $|\Delta\theta|$ to zero. Before proving the theorem, we develop the following Lemma.

Lemma Suppose

$$\dot{\theta} \leq \omega + u_0(A\theta + B), \quad (9)$$

where ω, u_0, A , and B are real constants. Then

$$\theta(t) \leq \frac{\omega + u_0 B}{u_0 A} \left(e^{u_0 A(t-t^*)} - 1 \right) + \theta(t^*) e^{u_0 A(t-t^*)} \quad (10)$$

for $t > t^*$.

Proof: Suppose equality held in (9), and make the substitution

$$\theta(t) = K(t) e^{u_0 A(t-t^*)}. \quad (11)$$

We solve the resulting differential equation for $K(t)$, using the fact that $\theta(t^*) = K(t^*)$ from (11) to determine the integration constant, to give

$$K(t) = \frac{\omega + u_0 B}{u_0 A} \left(1 - e^{-u_0 A(t-t^*)} \right) + \theta(t^*). \quad (12)$$

Then from (11),

$$\theta(t) = \frac{\omega + u_0 B}{u_0 A} \left(e^{u_0 A(t-t^*)} - 1 \right) + \theta(t^*) e^{u_0 A(t-t^*)}. \quad (13)$$

This is true when equality holds in (9). When the inequality holds, (13) gives an upper bound, implying (10). ■

This is a special case of Lemma 4.1.2 of [6], a form of Gronwall's Lemma. We can similarly show that if

$$\dot{\theta} \geq \omega + u_0(A\theta + B), \quad (14)$$

then for $t > t^*$ we have the bound

$$\theta(t) \geq \frac{\omega + u_0 B}{u_0 A} \left(e^{u_0 A(t-t^*)} - 1 \right) + \theta(t^*) e^{u_0 A(t-t^*)}. \quad (15)$$

We also note that if equality holds for (10) or (15) for $t > t^*$, then θ reaches the value $\tilde{\theta}$ at time

$$\tilde{t} = t^* + \frac{1}{u_0 A} \log \left(\frac{\omega + (B + A\tilde{\theta})u_0}{\omega + (B + A\theta(t^*))u_0} \right). \quad (16)$$

We now prove the theorem, maintaining the notational convenience of setting the time of the last spike $t_0 = 0$.

Proof: We begin by addressing the case

$$0 \leq \Delta\theta \leq \pi. \quad (17)$$

Piecewise linear outer and inner bounds for the phase response curve $Z_S(\theta) = -\sin(\theta)$ are

$$f_O(\theta) = \begin{cases} -\theta & 0 \leq \theta \leq \pi/2 \\ \theta - \pi & \pi/2 < \theta \leq 3\pi/2 \\ 2\pi - \theta & 3\pi/2 < \theta \leq 2\pi \end{cases} \quad (18)$$

$$f_I(\theta) = \begin{cases} -2\theta/\pi & 0 \leq \theta \leq \pi/2 \\ -2 + 2\theta/\pi & \pi/2 < \theta \leq 3\pi/2 \\ 4 - 2\theta/\pi & 3\pi/2 < \theta \leq 2\pi \end{cases}, \quad (19)$$

respectively. That is, we have

$$|f_I(\theta)| \leq |Z_S(\theta)| \leq |f_O(\theta)| \quad (20)$$

for all $\theta \in [0, 2\pi)$.

We will now find upper and lower bounds for $\theta(t)$ under the input (8) in the limit of small \bar{u} . Suppose that the neuron has just fired, so $\theta(0) = 0$. If there was no input ($\bar{u} = 0$), then $\theta(t_s/2) = \omega t_s/2 = \pi - (\Delta\theta)/4$, so that (17) implies that

$$3\pi/4 \leq \theta(t_s/2) \leq \pi. \quad (21)$$

Furthermore, $\theta(t_s) = \omega t_s = 2\pi - (\Delta\theta)/2$, so that (17) implies

$$3\pi/2 \leq \theta(t_s) \leq 2\pi. \quad (22)$$

It is always possible to choose \bar{u} sufficiently small so that these relationships hold even in the presence of input.

Let's first consider the upper bound for $\theta(t)$. Until θ reaches $\pi/2$, we have $\dot{\theta} \leq \omega + f_O(\theta)u_1 = \omega + \bar{u}\theta$. This gives the bound (10) with $t^* = 0, \theta(t^*) = 0, u_0 = \bar{u}, A = 1$, and $B = 0$. If equality held then, from (16), θ will be $\pi/2$ at time

$$t_{\pi/2} = \frac{1}{\bar{u}} \log \left(\frac{\omega + \pi\bar{u}/2}{\omega} \right). \quad (23)$$

Now, for $t_{\pi/2} < t < t_s/2$, we have $\dot{\theta} \leq \omega + f_O(\theta)u_1 = \omega + (\pi - \theta)\bar{u}$. The largest value that θ can reach by time $t_s/2$ is found by assuming equality, which from (13) with $t^* = t_{\pi/2}, \theta(t^*) = \pi/2, u_0 = \bar{u}, A = -1$, and $B = \pi$ gives

$$\theta_{max}(t_s/2) = -\frac{\omega + \bar{u}\pi}{\bar{u}} \left(e^{-\bar{u}(t_s/2 - t_{\pi/2})} - 1 \right) + \frac{\pi}{2} e^{-\bar{u}(t_s/2 - t_{\pi/2})}. \quad (24)$$

From (21), for sufficiently small \bar{u} we expect that $\theta_{max}(t_s/2) \leq \pi$. Until θ reaches π , the PRC $Z_S(\theta)$ is negative and $u(t) = \bar{u}$ is positive (since $t > t_s/2$). Thus $\dot{\theta} \leq \omega + f_I(\theta)u_2 = \omega + (\frac{2}{\pi}\theta - 2)\bar{u}$. This gives the bound (10) with $t^* = t_s/2, \theta(t^*) = \theta_{max}(t_s/2), u_0 = \bar{u}, A = 2/\pi, B = -2$. If equality held, then from (16), $\theta = \pi$ at time

$$t_\pi = t_s/2 + \frac{\pi}{2\bar{u}} \log \left(\frac{\omega}{\omega + 2(\theta_{max}(t_s/2)/\pi - 1)\bar{u}} \right) \quad (25)$$

Now, until θ reaches $3\pi/2$, we have $\dot{\theta} \leq \omega + f_O(\theta)u_2 = \omega + (\theta - \pi)\bar{u}$. If equality held, the time to reach $\theta = 3\pi/2$ is found from (16) with $t^* = t_\pi, \theta(t^*) = \pi, u_0 = \bar{u}, A = 1, B = -\pi$:

$$t_{3\pi/2} = t_\pi + \frac{1}{\bar{u}} \log \left(\frac{\omega + \pi\bar{u}/2}{\omega} \right). \quad (26)$$

Finally, until θ reaches 2π , we have $\dot{\theta} \leq \omega + f_O(\theta)u_2 = \omega + (2\pi - \theta)\bar{u}$. If equality held, the time to reach $\theta = 2\pi$ is found from (16) with $t^* = t_{3\pi/2}$, $\theta(t^*) = 3\pi/2$, $u_0 = \bar{u}$, $A = -1$, $B = 2\pi$:

$$t_{2\pi} = t_{3\pi/2} + \frac{1}{\bar{u}} \log \left(\frac{\omega + \pi\bar{u}/2}{\omega} \right). \quad (27)$$

A similar argument can be made to show that for the lower bound of $\theta(t)$, using similar notation,

$$\begin{aligned} t'_{\pi/2} &= \frac{\pi}{2\bar{u}} \log \left(\frac{\omega + \bar{u}}{\omega} \right), \\ \theta_{min}(t_s/2) &= -\frac{\pi(\omega + 2\bar{u})}{2\bar{u}} \left(e^{-2\bar{u}(t_s/2 - t_{\pi/2})/\pi} - 1 \right) \\ &\quad + \frac{\pi}{2} e^{-2\bar{u}(t_s/2 - t_{\pi/2})/\pi}, \\ t'_\pi &= \frac{t_s}{2} + \frac{1}{\bar{u}} \log \left(\frac{\omega}{\omega + (\theta_{min}(t_s/2) - \pi)\bar{u}} \right), \\ t'_{3\pi/2} &= t_\pi + \frac{\pi}{2\bar{u}} \log \left(\frac{\omega + \bar{u}}{\omega} \right). \end{aligned}$$

The input $u(t)$ must be nonnegative for $3\pi/2 < \theta < 2\pi$ (from (21), it can only be negative up to $\theta = \pi$). But from (22), we cannot guarantee that the input will be nonzero for this range of θ values. $Z_S(\theta)$ is positive for this range, so the worst case scenario for our lower bound is zero input for $3\pi/2 < \theta < 2\pi$, giving

$$t'_{2\pi} = t_{3\pi/2} + \frac{\pi}{2\omega}.$$

Our reference trajectory is $\theta_r(t) = \Delta\theta + \omega t$, so $\theta_r(t_{2\pi}) = \Delta\theta + \omega t_{2\pi}$. Our phase error at $t_{2\pi}$ is then

$$\Delta\theta^{new} = \theta_r(t_{2\pi}) - 2\pi. \quad (28)$$

Let $\bar{u} = c\Delta\theta$, where $c > 0$. Using the above formulae, and expanding around $c = 0$, for our upper bound for $\theta(t)$ we find

$$\frac{\Delta\theta^{new}}{\Delta\theta} = 1 + \underbrace{\frac{(\Delta\theta)^2(2 + \pi) - 16\pi^3}{32\pi\omega}}_{g_u(\Delta\theta)/\omega} c + \mathcal{O}(c^2). \quad (29)$$

For our lower bound for $\theta(t)$ with small c ,

$$\frac{\Delta\theta^{new}}{\Delta\theta} = 1 + \underbrace{\frac{(\Delta\theta)^2(2 + \pi) - 24\pi^2}{32\pi\omega}}_{g_l(\Delta\theta)/\omega} c + \mathcal{O}(c^2). \quad (30)$$

where $g_u(\theta) < 0$ and $g_l(\theta) < 0$ for initial error satisfying (17). Furthermore, choosing c sufficiently small, $\Delta\theta^{new} \geq 0$. Therefore, our control algorithm, in the limit of small \bar{u} , decreases the error each iteration.

A similar argument can be made for $-\pi \leq \Delta\theta < 0$. Alternatively, suppose $u(t) = \epsilon v(t)$ and $\theta(t) = \omega t + \epsilon\theta_1(t) + \mathcal{O}(\epsilon^2)$. Then

$$\begin{aligned} \theta(t) &= \int_0^t [\omega + f(\theta(t'))u(t')] dt' \\ &= \omega t + \epsilon \int_0^t f(\omega t')v(t') dt' + \mathcal{O}(\epsilon^2). \end{aligned}$$

For $v(t) = \pm\bar{v}$,

$$\theta(t) = \omega t \pm \epsilon\bar{v} \int_0^t f(\omega t') dt' + \mathcal{O}(\epsilon^2). \quad (31)$$

That is, a small, positive constant input advances the phase by the same amount that a small, negative constant input of the same magnitude retards the phase. For the input (8), we thus get the same bounds for $-\pi \leq \Delta\theta < 0$. ■

As implied above, an equivalent condition to global monotonic convergence of the phase error $|\Delta\theta|$ to zero is the phase error gain $|\Delta\theta^{new}/\Delta\theta| < 1$ over the full measure of the domain $(-\pi, \pi]$. Figure 2(a) shows results from simulation that verify the global monotonic phase error convergence for the case when $c = 0.05$ and $\omega = 1$.

Another tool to analyze stability of the system is the one dimensional map $M : (-\pi, \pi] \rightarrow (-\pi, \pi]$ defined by $\Delta\theta^{new} = M(\Delta\theta)$. Figure 2(b) shows that, for this case, the fixed point of M at $\Delta\theta = 0$ for this case is clearly globally stable since the origin is a stable fixed point and the absolute value of the slope is bounded by one over the entire domain.

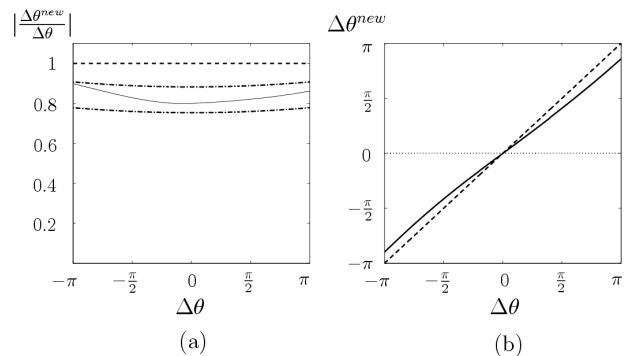


Fig. 2. Numerical results for the proportional control law as described in (8) with $c = 0.05$. The solid line in (a) is the phase error gain, shown within the bounds (30) and (29). Figure (b) shows the final error map M displayed as a solid line with the dashed line $\Delta\theta^{new} = \Delta\theta$ where intersections correspond to a fixed point.

IV. GLOBAL ASYMPTOTIC STABILITY

The global monotonic convergence of $|\Delta\theta|$ to zero, as described above, is a strong form of global stability that may not be attainable for all oscillators with phase response curves in the family we wish to consider. Also, in the limit of small control magnitudes, slow monotonic convergence may not be as desirable as fast asymptotic convergence in the context of controlling neural synchrony.

These caveats lead us to investigate the concept of relaxing the monotonicity requirement, and instead focusing on asymptotic stability of a control scheme. Given a constant frequency reference trajectory θ_r , as defined in (4), global asymptotic stability on \mathbb{S}^1 can be ascertained by analyzing the stability of the fixed point at $\Delta\theta = 0$ of the map M , as defined in the previous section.

For a phase oscillator subject to the control algorithm based only on the error $\Delta\theta = \theta_r - \theta$ computed at a marker event on its closed orbit, $\Delta\theta$ globally converges to zero if

the map M has a single stable fixed point at $\Delta\theta = 0$ with a basin of attraction consisting of the full measure of the interval $(-\pi, \pi]$. This, however, is only a sufficient condition for global stability. In the next section, we will show results from a control law developed for the Hodgkin-Huxley phase reduction model that show global asymptotic stability on a set of full measure, but do not exhibit monotonic error convergence.

Unfortunately, the development closed-form analytic representations of the map M may not be tractable, in general. However, maps of this type are easily approximated by simulation. By sampling a discrete set of $\Delta\theta$ points throughout the domain, applying the control law and observing $\Delta\theta^{new}$ at the time of the next marker event, an approximation of the map M can be constructed of arbitrary (finite) resolution. This is the method we have used to construct the results presented earlier in Figure 2, as well as the forthcoming results in the next section. Once a sufficiently accurate approximation of M has been calculated, the basin of attraction of the stable fixed point at the origin (which, by construction will exist) can be easily ascertained by graphical methods, e.g. *cobwebbing* [12], or by reformulating the map as a Markov process and checking the state transition operator for a single eigenvalue of 1 with an eigenvector representing the origin.

V. EXTENSION OF THE CONTROL LAW

We now develop a heuristic method for calculating reasonable control magnitudes for a more general class of phase response curves. The control objective will be to reduce the phase error as much as possible within one period of the neuron, which implies a preference for fast asymptotic convergence over slow monotonic convergence. We propose a control law that will provide stimulus through the entire duration of the desired period, which is a more aggressive strategy than the similar control law developed earlier in (8). In addition, we forego the strict requirement of charge balance, in favor of waveforms that are “nearly” charge-balanced. This is acceptable because small deviations in charge balance can be easily computed and corrected by applying a short corrective pulse when the neuron fires (since the PRC is zero at $\theta = 0$, a short corrective pulse will have no effect on the dynamics). To simplify the presentation, we will neglect this technicality.

We no longer assume the symmetric form of a sinusoidal waveform, instead we consider smooth phase response curves derived from systems exhibiting a Hopf (or Bautin) bifurcation, which yield a class characterized by the conditions

$$\begin{aligned} Z(0) &= 0, & Z'(0) &< 0 \\ Z(\alpha) &= 0, & Z'(\alpha) &> 0 \\ \max(Z(\theta)) &> 0, & \min(Z(\theta)) &< 0. \end{aligned} \quad (32)$$

For such a phase model, the control waveform may be parametrized as follows:

$$u(t) = \begin{cases} \bar{u}_1, & \text{for } t_0 \leq t < t_0 + t_{\text{switch}} \\ \bar{u}_2, & \text{for } t_0 + t_{\text{switch}} \leq t < t_0 + t_r \\ 0, & \text{otherwise} \end{cases} \quad (33)$$

where $t_{\text{switch}} = (\frac{\alpha}{2\pi})t_r$, and $t_r = \frac{2\pi - \Delta\theta}{\omega}$ is the time the reference trajectory crosses zero. Suitable values for \bar{u}_1 and \bar{u}_2 can be approximated by the following:

$$\bar{u}_1 = \frac{2\pi\omega\Delta\theta}{\alpha(2\pi - \Delta\theta)(\bar{Z}_1 - \bar{Z}_2)} \quad (34)$$

$$\bar{u}_2 = \frac{-2\pi\omega\Delta\theta}{(2\pi - \alpha)(2\pi - \Delta\theta)(\bar{Z}_1 - \bar{Z}_2)}. \quad (35)$$

Here, $\bar{Z}_1 = \frac{1}{\alpha} \int_0^\alpha Z(\theta) d\theta$ $\bar{Z}_2 = \frac{1}{2\pi - \alpha} \int_\alpha^{2\pi} Z(\theta) d\theta$.

We arrive at (34) and (35) by considering the average values \bar{Z}_1 and \bar{Z}_2 of the two intervals of the phase response curve $Z(\theta)$. We will use the simplifying assumption of linear phase evolution proportional to the length of the intervals, i.e. $\theta = \alpha$ at time $t_0 + t_{\text{switch}}$, and $\theta = 2\pi$ at time $t_0 + t_r$.

Using the square waveform, the charge-balance equation

$$\int_{t_0}^{t_0 + t_r} u(t) dt = 0 \quad (36)$$

yields the following relation:

$$\frac{\alpha}{2\pi}\bar{u}_1 + (1 - \frac{\alpha}{2\pi})\bar{u}_2 = 0. \quad (37)$$

Approximating $Z(\theta)$ by \bar{Z}_i for $\theta \in I_i$ gives a simple separable ODE with the following solution

$$2\pi = \omega t_r + \bar{u}_1 \bar{Z}_1 \frac{\alpha}{2\pi} t_r + \bar{u}_2 \bar{Z}_2 \left(1 - \frac{\alpha}{2\pi}\right) t_r. \quad (38)$$

Without loss of generality, we take $t_0 = 0$ and it is readily shown that (34) and (35) are the solution in terms of \bar{u}_1 and \bar{u}_2 .

Both control laws (8) and (33) use a piecewise constant waveform that switches sign during the period of actuation and switches to zero afterward. They differ in the way the magnitudes are calculated given the phase error $\Delta\theta$, and, more subtly, in their switching times. Since the simple phase oscillator with the PRC $Z_S(\theta) = -\sin(\theta)$ has $\bar{Z}_1 = -\bar{Z}_2$, and thus $\bar{u}_1 = -\bar{u}_2$, we can parameterize the control magnitude by a single variable, $\bar{u} = \bar{u}_2 = -\bar{u}_1$, and directly compare the two methods.

Given their slightly different switching time schemes, the goal of these methods is to calculate the best control magnitude, \bar{u} , as a function of initial error, $\Delta\theta$. Recall that the control law (8) uses $\bar{u} = c\Delta\theta$ where $0 < c \ll 1$, while the control law (33) uses (34) and (35). To ascertain the effectiveness of the two methods, we fix the control magnitude, \bar{u} , and simulate a single period of control to get the phase error gain $|\Delta\theta^{new}/\Delta\theta|$ for a specific initial phase error $\Delta\theta$. Repeating over a set of initial phase errors $\Delta\theta \in [-\pi, \pi)$ shows the effectiveness of that particular \bar{u} value as a function of the initial phase error. Performing these simulations over a set of $\bar{u} \in [-2, 2]$ quantifies the performance over a range of \bar{u} values as a function of initial error. In these plots, shown for both schemes in Figure 3, we have truncated values over 1 (so they appear white) to better visualize the regions of good controller performance (small $|\Delta\theta^{new}/\Delta\theta|$). Figure 3(a) shows results using the timing scheme from (8) and one can see that a line $\bar{u} = c\Delta\theta$

for small positive c will lie entirely within the region of negative phase error gain. Figure 3(b) shows results using the timing scheme from (33) and one can see that the white dashed curve calculated by (34) and (35) lies over the region of lowest error gain. Using this control, we observe a very low gain curve and extremely stable error map, as shown in Figures 3(c) and 3(d), compared with the results from the less aggressive scheme shown in Figure 2.

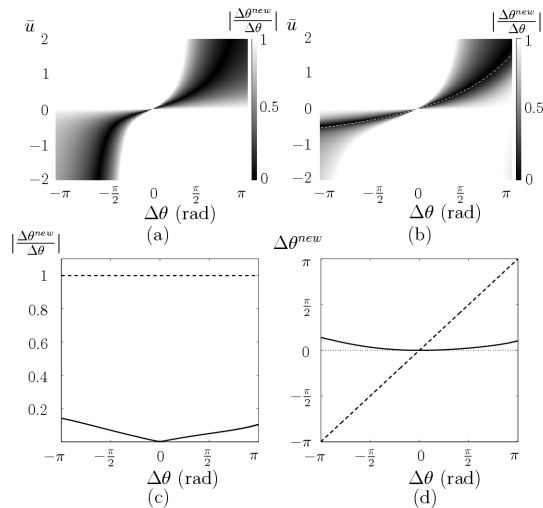


Fig. 3. Phase error gain for the PRC $Z_S(\theta) = -\sin(\theta)$ for the control scheme from (a) Eqn. (8) and (b) Eqn. (33) with different values of \bar{u} , and (c) Eqn. (33) using (34) and (35). (d) shows the map M corresponding to (c). The white dashed line in (b) corresponds to the results shown in (c) and (d).

We now consider the phase reduction of the Hodgkin-Huxley system, with the phase response curve shown previously in Figure 1. For this system, $\alpha \approx 4.12$, $\bar{Z}_1 \approx -0.031$, $\bar{Z}_2 \approx 0.105$. Again, by simulation we study both the gain and final error map. Figure 4(a) shows that this system does not have monotonic gain convergence, but the stable fixed point at the origin of the map M does have a basin of attraction consisting of the entire domain (less the unstable fixed point, a set of zero measure), so the system with the proposed control scheme is asymptotically stable.

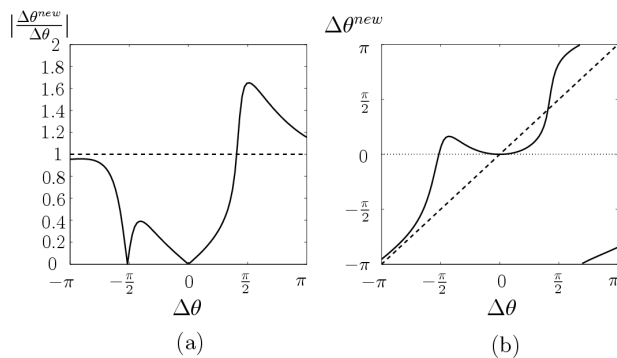


Fig. 4. (a) Phase error gain and (b) map M for the Hodgkin-Huxley PRC for the control scheme from Eqn. (33) using (34) and (35).

VI. CONCLUSIONS

In this paper, we introduced a control problem drawn from electrical deep brain stimulation, a treatment for neurolocal disorders. We proposed novel feedback control mechanisms which control the phase of an individual neuron, assuming only that the phase response curve is known and that the time at which the neuron fires can be detected. The effectiveness of this mechanism was demonstrated through analytical and numerical results. For a population of uncoupled neurons, appropriate application of this control scheme to each individual oscillator will desynchronize the population, as desired.

There are many extensions to the present work that we plan to consider, including controlling individual neurons with Type I phase response curves, such as the Hindmarsh-Rose model [2], commanding individual neurons to fire at frequencies different from their natural frequency, and desynchronizing coupled populations of neurons. We also plan to broaden the class of waveforms we consider to take advantage of the properties of the phase response curve in order to minimize the total delivered energy, and will compare with results from optimal open-loop techniques [10].

REFERENCES

- [1] A. L. Benabid, P. Pollak, C. Gervason, D. Hoffmann, D. M. Gao, M. Hommel, J. E. Perret, and J. De Rougemont. Long-term suppression of tremor by chronic stimulation of the ventral intermediate thalamic nucleus. *The Lancet*, 337:403–406, 1991.
- [2] E. Brown, J. Moehlis, and P. Holmes. On the phase reduction and response dynamics of neural oscillator populations. *Neural Comp.*, 16:673–715, 2004.
- [3] P. Danzl, R. Hansen, J. Moehlis, and G. Bonnet. Partial phase synchronization of neural populations due to random Poisson inputs. 2007. Submitted to *J. Comp. Neurosci.*
- [4] L. Glass. Synchronization and rhythmic processes in physiology. *Nature*, 410:277–284, 2001.
- [5] J. Guckenheimer. Isochrons and phaseless sets. *J. Math. Biol.*, 1:259–273, 1975.
- [6] J. Guckenheimer and P. J. Holmes. *Nonlinear Oscillations, Dynamical Systems and Bifurcations of Vector Fields*. Springer-Verlag, New York, 1983.
- [7] A. L. Hodgkin and A. F. Huxley. A quantitative description of membrane current and its application to conduction and excitation in nerve. *J. Physiol.*, 117:500–544, 1952.
- [8] J. Keener and J. Sneyd. *Mathematical Physiology*. Springer, New York, 1998.
- [9] Y. Kuramoto. *Chemical Oscillations, Waves, and Turbulence*. Springer, Berlin, 1984.
- [10] J. Moehlis, E. Shea-Brown, and H. Rabitz. Optimal inputs for phase models of spiking neurons. *J. Comp. and Nonlin. Dyn.*, 1(4):358–367, 2006.
- [11] D. Pare, R. Curro’Dossi, and M. Steriade. Neuronal basis of the Parkinsonian resting tremor: a hypothesis and its implications for treatment. *Neuroscience*, 35:217–226, 1990.
- [12] S.H. Strogatz. *Nonlinear Dynamics and Chaos: With Applications to Physics, Biology, Chemistry, and Engineering*. Perseus Books, Cambridge, MA, 1994.
- [13] P. Tass, J. Klosterkötter, F. Schneider, D. Lenartz, A. Koulousakis, and V. Sturm. Obsessive-compulsive disorder: Development of demand-controlled deep brain stimulation with methods from stochastic phase resetting. *Neuropsychopharmacology*, 28:S27–S34, 2003.
- [14] P. A. Tass. *Phase Resetting in Medicine and Biology*. Springer, New York, 1999.
- [15] A. Winfree. Patterns of phase compromise in biological cycles. *J. Math. Biol.*, 1:73–95, 1974.
- [16] A. Winfree. *The Geometry of Biological Time, Second Edition*. Springer, New York, 2001.